Oil Shale, 2018, Vol. 35, No. 3, pp. 242–253
doi: https://doi.org/10.3176/oil.2018.3.04
ISSN 0208-189X

FLOTATION COLLECTOR PREPARATION AND EVALUATION OF OIL SHALE

LIJUN LIU[(a)], GAN CHENG[(b,c)*], WEI YU[(a)], CHAO YANG[(a)]

(a) School of Chemistry and Chemical Engineering, Xi'an University of Science and Technology, Xi'an 710054, PR China
(b) College of Chemistry and Chemical Engineering, Henan Polytechnic University, Jiaozuo 454000, PR China
(c) Henan Key Laboratory of Coal Green Conversion, Henan Polytechnic University, Jiaozuo 454000, PR China

Abstract. *As the world's second largest solid fossil fuel deposit after coal, utilization of oil shale has become a research hotspot lately. The application of oil shale may be limited because of its high ash content. In this paper, froth flotation technology was used to treat oil shale. Oil shale samples were characterized by ultimate and proximate analyses. The collector was prepared using mechanical stirring and ultrasonic cell crusher methods. The dispersion of synthetic collectors was measured. When the mass ratio of kerosene to oleic acid was 1:1 and the agitation speed was 1800 rpm (hereinafter referred to as synthetic collector A), the dispersion property of the synthetic collector was the best, and the flotation results indicated that the flotation effect of synthetic collectors was improved. Collector adsorption measurements indicated that with increasing collector dosage, the adsorption quantity first increased and then leveled off at a dosage of 500 g/t. The infrared spectra of raw oil shale, kerosene, oleic acid and synthetic collector A were measured and the interactions between them were analyzed. The reasons for the good performance of synthetic collector A were found out.*

Keywords: *raw oil shale, froth flotation, synthetic collector, ash content, recovery, separation.*

1. Introduction

With the exhaustion of petroleum resources and the growing energy demand due to the world economic progress, the development of substitute resources has become urgent. China's resource of oil is insufficient and its production is far from satisfying the social and economic needs of the country. In 2016, China imported about 376 million tons of crude oil, the degree of external

* Corresponding author: email *chenggan464@126.com*

dependence making 65.5%. Oil strategic security issues have been given more and more prominence these years. China's overall oil shale reserves are estimated at 4.76×10^{10} tons and could significantly increase petroleum supply [1].

Pyrolysis is the main method to transform oil shale into shale oil. The oil shale pyrolysis process involves complex physical and chemical reactions. Lots of treatment processes and methods for oil shale pyrolysis have been carried out in order to enhance the yield of oil and improve its quality [2]. By this, parameters such as composition of source material, pyrolysis temperature, heating rate, residence time and particle size are taken into account [3, 4]. Pyrolysis under vacuum conditions has been shown to improve both the yield and quality of oil unlike pyrolysis under atmospheric pressure. Vacuum pressures accelerate the transport of pyrolysis products by affording a faster escape of primary oil from the reaction zone, therefore reducing the occurrence of secondary cracking reactions [5].

Oil shale, as a humic sludge substance, has not only some basic properties of coal but also unique properties of its own. Oil shale is characterized by a high content of ash and a low amount of organic matter compared to coal [6]. Generally, the amount of organic matter in oil shale is less than 35%, while that in coal is more than 75%. The H-to-C atomic ratio of oil shale is higher than that of coal. The amount of minerals is high in oil shale, which after the thermal decomposition go over to semicoke. As a result, the ash content of semicoke becomes higher and its calorific value lower than oil shale's, which reduces the economic value of semicoke and restrains its use [7]. Therefore, it is beneficial to reduce the ash content in oil shale by using the flotation technique [8].

Flotation is an easy and effective way to upgrade minerals [9]. The technique has been widely used in various fields, such as maceral separation, mineral separation, oil-water separation, paper pulp deinking, waste water treatment, etc. Utilization of oil shale in China will benefit from reducing its ash content via flotation [10]. One of the flotation research focuses is on selecting suitable reagents to improve oil shale flotation performance. However, up to now, only a few articles have touched upon oil shale flotation. Altun et al. [11] used the froth flotation technique to upgrade Turkish low-quality oil shale by employing amine-type collectors. It was found that ash could be reduced from 69.88% to 53.10% with a 58.64% combustible recovery, using an 800 g/ton Armoflote17 (AkzoChemical, Netherlands) at a neutral pulp pH. Altun et al. [12] further attempted to enhance the performance of flotation cleaning of oil shales by use of ultrasound. The results showed that the ultrasonic treatment increased the extent of ash rejection. After the ultrasonic treatment, the ash content of Himmetoğlu oil shale decreased from 34.76% to 11.82% with an 82.66% combustible recovery, and that of Beypazarı oil shale decreased from 69.88% to 34.76% with a 64.78% combustible recovery.

In this work, the flotation collector was synthesized by mechanical stirring and ultrasonic treatment. The optimal collector design and preparation conditions were found out. The study of the mechanism of interaction between the collector and mineral is useful to understand the structure and performance of the synthetic collector, so as to optimize and adjust the flotation conditions to achieve a higher degree of separation by flotation. In the current paper, the performance of synthetic collector A was studied by measuring the amount of adsorption by infrared spectroscopy. A single collector refers to kerosene or oleic acid, the synthetic collectors refer to the reagents synthesized by two or more reagents.

2. Experiment

2.1. Materials and instruments

The oil shale sample used in this paper was collected from Qingchuan mining district in Sichuan Province, China. The flotation experiments were carried out in a conventional mechanical flotation cell. The details about the equipment used (all China) are given in Table 1.

Table 1. Equipment details

Equipment	Producer	Model
Flotation machine	Jilin Prospecting Machinery Factory	XFD_{IV}-1.5L
Vacuum filter	Wuhan Rock Crush & Grand Equipment Manufacture Co., Ltd	RK/ZL-ø260/ø200
Thermostatic drying oven	Tianjin Taisite Instrument Co., Ltd	101-3AB
Muffle furnace	Test Center of China Coal Research Institute	GW 300C
Double Beam UV Visible Spectrophotometer	Beijing Purkinje General Instrument Co., Ltd	TU-1900
Ultrasonic cell disruptor	Ningbo Scientz Biotechnology Co., Ltd	JY 92-IIN

2.2. Ultimate and proximate analyses

The results of ultimate analysis of the oil shale sample showed that the contents of nitrogen, carbon and protium were 0.86%, 58.62% and 5.59%, respectively, indicating that the organic matter in it was abundant. The ratio of the number of carbon atoms to hydrogen atoms was 9:10, and was close to that of aromatic hydrocarbons, indicating that oil shale contained a lot of substantial benzene rings [13].

The results of proximate analysis of the sample demonstrated that its volatile content was 51.18% and that of ash 29.82%. Generally, the high volatile and low ash contents imply a high concentration of oil, which means that oil shale has a high utilizing value.

Table 2. Particle size distribution analysis of the oil shale sample

Particle size, μm	Product yield, %	Ash, %	Cumulative oversize, %	
			Product yield	Ash
500	1.54	25.03	1.54	25.03
–500 to +250	16.32	26.61	17.86	26.47
–250 to +125	32.65	26.55	50.51	26.52
–125 to +75	22.63	28.55	73.14	27.15
–75 to +45	8.47	31.82	81.6	27.63
–45	18.4	37.56	100	29.46
Total	100	29.46	—	—

Note: "–" represents no data.

From Table 2 it can be seen that the ash content of the sample slightly increased with decreasing particle size. The increase was particularly significant in case of –75 μm fractions. In case of –45 μm fractions, the product yield was 18.40 %. Particles with a size of –250 to +75 μm accounted for 55.28% of the total mass of the sample.

2.3. Experimental methods

Using kerosene and oleic acid as raw materials, synthetic collectors were prepared by mechanical stirring and ultrasonic treatment. During the experiment, the proportion between the two components and the instrument power were the two critical parameters. After the stability of the synthetic collector was measured, the optimal collector was used in flotation experiments.

The quantitative analysis methods included phase-resolved ultraviolet (UV) spectrophotometry and two-phase titration method [14, 15]. In this study, phase-resolved UV spectrophotometry was used to find the residual concentration of the flotation collector after adsorption by the mineral, and then the amount of the collector adsorbed on the mineral surface was calculated by the following formula [16]:

$$A = \frac{(\rho_0 - \rho_X)v}{m}, \tag{1}$$

where A is the amount of adsorption, mg/g; ρ_0 is the initial concentration of solution, mg/L; ρ_x is the concentration of solution after adsorption, mg/L; V is the volume of solution, L; m is the mass of solid, g.

3. Results and discussion

3.1. Synthesis of the collector

It was observed that when the ratio of kerosene to oleic acid was 1:1 and the agitation speed 1800 rpm, the synthetic collector was the most stable.

Table 3. Collector preparation by mechanical stirring

Kerosene:oleic acid ratio	Stirring time, h	Stirring speed, rpm	Observations after 3-day standing
1:1	1	1100	Stratification
		1800	Foam layer, no stratification
		2500	Stratification
1.5:1	1	1100	Stratification
		1800	Slight stratification
		2500	Slight stratification
1:1.5	1	1100	Obvious stratification
		1800	Foam layer, obvious stratification
		2500	Foam layer, obvious stratification

Table 4. Collector preparation by ultrasonic cell crusher

Kerosene:oleic acid ratio	Processing time, h	Power, W	Observations after 3-day standing
1:1	1	10	Existence of sediments
		20	Abundance of sediments
		30	Existence of sediments
1.5:1	1	10	Absence of sediments
		20	Absence of sediments
		30	Absence of sediments
1:1.5	1	10	Abundance of sediments
		20	Abundance of sediments
		30	Abundance of sediments

A comparison of the results presented in Tables 3 and 4 showed that the higher the proportion of kerosene in the solution, the higher its stability. When the kerosene-to-oleic acid ratio was 1.5:1, no sediments existed in the three kinds of solutions. When the respective ratio was 1:1.5, the sediments were present in a maximal amount, and kerosene and oleic acid were almost completely separated. So, at a 1.5:1 ratio of kerosene to oleic acid and the instrument power of 10 W, the synthetic collector was the most stable.

For dispersion measurements, better-performing stable reagents, labeled as A and B, were used. The kerosene:oleic acid ratio of reagent A was 1:1 and the agitation speed 1800 rpm, while reagent B had the kerosene:oleic acid ratio of 1.5:1 and the instrument power of 10 W.

The synthetic collectors were separately added to 200 mL of water, then stirred mechanically for 30 min and thereafter ultrasonically for 30 min. Finally, a Malvern Zetasizer Nano ZS90 particle-size zeta-potential analyzer (UK) was used to measure the particle size of the synthetic collector in the solution to evaluate its dispersion. The particle size of synthetic collector A was minimal, only 295 nm, while that of synthetic collector B was 433.2 nm. At the same time, the dispersion of collector A was the best, in terms of non-polar agents.

3.2. Flotation results

Octanol was used as the frother, with a dosage of 200 g/t. The collector dosages were 400, 500 and 600 g/t. The aeration rate was 0.12 m³/h and the oil shale ore mass 100 g. The flotation results are presented in Table 5.

Table 5. Flotation performance of synthetic collector A

Collector dosage, g/t	Product	Product yield, %	Ash, %	Recovery, %
600	Concentrate	96.41	24.52	98.80
	Tailing	3.59	75.45	1.20
500	Concentrate	95.94	23.18	98.74
	Tailing	4.06	76.85	1.26
400	Concentrate	95.27	23.64	98.49
	Tailing	4.73	76.36	1.51

Table 5 reveals that the yield of the concentrate was the highest when the collector dosage was 600 g/t, and the lowest when the respective dosage was 400 g/t. The ash content of the concentrate was the highest at the collector dosage of 600 g/t and the lowest at 500 g/t. The recovery rates at collector dosages of 500 and 600 g/t were nearly equivalent. These results demonstrated that the collector dosage of 500 g/t was the most optimal.

Next, kerosene and oleic acid were used as collectors and octanol as the frother. The collector dosage was 500 g/t and that of the frother 200 g/t. The aeration rate was 0.12 m³/h and the oil shale ore mass 100 g. The results are given in Table 6.

From Tables 5 and 6 it can be seen that the flotation concentrate ash contents of the single collector were mostly higher than those of the synthetic collector, and the flotation concentrate yields were lower than those of the synthetic collector. These results gave evidence of that the flotation effect of the single collector was poor.

In the next experiment, kerosene and oleic acid were used as collectors and octanol as the frother. The frother dosage was 200 g/t and the collector dosages were 400, 500 and 600 g/t. Kerosene and oleic acid were added at a 1:1 ratio. The aeration rate was 0.12 m³/h and the oil shale ore mass 100 g. The results are given in Table 7.

Table 6. Flotation performance of the single collector

Collector	Product	Product yield, %	Ash, %	Recovery, %
Kerosene	Concentrate	87.46	24.41	94.27
	Tailing	10.93	77.95	3.44
Oleic acid	Concentrate	68.90	25.31	86.73
	Tailing	31.10	74.69	13.27

Table 7. Flotation results after addition of kerosene and oleic acid

Collector dosage, g/t	Product	Product yield, %	Ash, %	Recovery, %
400	Concentrate	88.77	24.99	95.83
	Tailing	11.23	74.21	4.17
500	Concentrate	91.18	25.97	96.78
	Tailing	8.82	74.56	3.22
600	Concentrate	91.23	26.62	96.73
	Tailing	8.77	74.22	3.27

A comparison of the data given in Tables 5 and 7 shows that after addition of kerosene and oleic acid as collectors, their flotation concentrate ash contents were higher and concentrate yields lower than those of the synthetic collector.

So, the flotation performance of synthetic collectors was better.

3.3. Collector adsorption measurement

The experimental adsorption quantity data are shown in Figure 1.

It can be seen from Figure 1 that the quantity of adsorption of the collector on the oil shale surface increased with increasing collector dosage, and reached a relatively stable value at a collector dosage of 500 g/t.

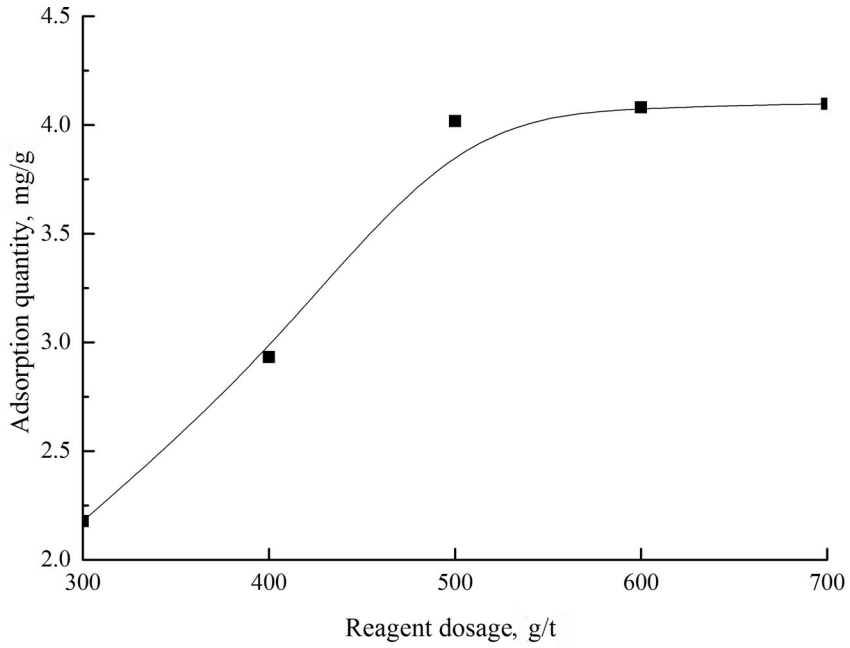

Fig. 1. Adsorption quantity at different collector dosages.

3.4. Infrared spectroscopic analysis

The sample solution was prepared using a certain amount of oil shale and 500 g/t of the collector. Some water was added to obtain the solution concentration of 60 g/L. The samples were obtained by stirring the solution for 30 min, filtering through a funnel, rinsing with distilled water, and, finally, drying [17]. The Fourier transform infrared (FTIR) spectra were obtained between 4000 and 400 cm^{-1}.

The FTIR spectra of raw oil shale, kerosene and kerosene-infiltrated oil shale in Figure 2 illustrate the interaction between them.

The peaks in the range 4000–2800 cm^{-1} in Figure 2a correspond to the stretching vibrations of OH, NH and NH_2 groups of phenol and alcohol. The broad band at 3480 cm^{-1} shows the presence of dissociative NH_2 and hydroxyl OH groups. The double adsorption band at 2920 cm^{-1} is due to the presence of CH_2. The peak at 2340 cm^{-1} is attributable to carboxylic acid. The adsorption band at 1440 cm^{-1} indicates the unsaturated =C–H group. In addition, the adsorption band at 1030 cm^{-1} denotes that an aliphatic C–H group exists in this adsorption band.

The double adsorption bands at 3000 cm^{-1} and 2920 cm^{-1} in Figure 2b are due to the presence of CH_2, indicating the carbon-chain or cycloalkane structure of kerosene. The bands at 1460 cm^{-1} and 1380 cm^{-1} are due to the

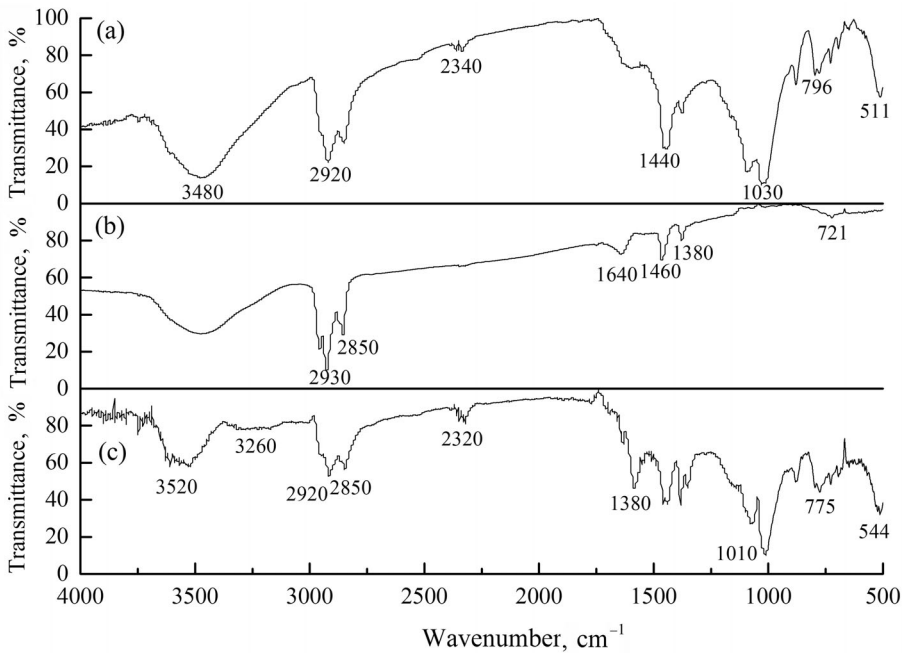

Fig. 2. FTIR spectra of (a) raw oil shale, (b) kerosene, (c) oil shale infiltrated by kerosene.

deformation vibration of alkane or the stretching vibration of olefin. The adsorption band at 1640 cm^{-1} signifies the stretching vibration of unsaturated olefin.

In Figure 2c, there are several new significant absorption peaks on the FTIR spectrum of the oil shale infiltrated by kerosene, in addition to the corresponding bands of minerals. For example, the adsorption band at 3520 cm^{-1} is due to the consociation of hydroxyl and amino.

In Figure 3, the FTIR spectra of raw oil shale, oleic acid and oleic acid-infiltrated oil shale illustrate the interaction between them.

For Figure 3a, see the description above pertaining to Figure 2a. In Figure 3b, the broad band at 3630 cm^{-1} belongs to the stretching vibration of the OH group. The absorption peaks at 3030 cm^{-1}, 2920 cm^{-1} and 2850 cm^{-1} are attributable to the deformation vibration of CH_3 and CH_2 groups. The peak at 1710 cm^{-1} shows the stretching vibration of the C=O group. The strong band at 1280 cm^{-1} is indicative of the presence of the stretching vibration of the C–O group and the deformation vibration of the O–H group, which conform to the respective vibrations of the alkyl and carboxylic functional groups of oleic acid.

From Figure 3c it can be seen that there have appeared several new absorption peaks on the FTIR spectrum of oil shale infiltrated by oleic acid, in addition to the corresponding bands of minerals. The peaks at about

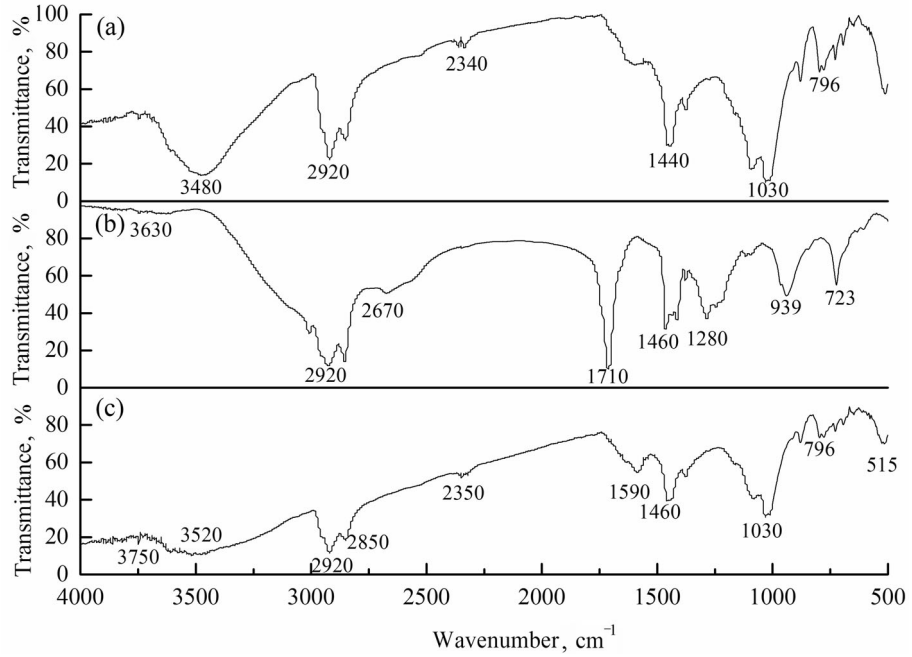

Fig. 3. FTIR spectra of (a) raw oil shale, (b) oleic acid, (c) oil shale infiltrated by oleic acid.

1400 cm^{-1} and 2300–2380 cm^{-1} are attributable to chlorite, talc, epidote, hornblende, etc. The FTIR spectra in the figure include not only the absorption peaks of raw oil shale but also those of oil shale infiltrated by oleic acid. For example, the adsorption band at 1740 cm^{-1}, which is assignable to the stretching vibration of the C=O group, implies that oil shale absorbs a small amount of oleic acid.

In Figure 4, the FTIR spectra of raw oil shale, synthetic collector A and oil shale infiltrated by synthetic collector A illustrate the interaction between them.

For Figure 4a, see the description above relating to Figure 2a. The adsorption bands at 3030 cm^{-1}, 2920 cm^{-1} and 2820 cm^{-1} in Figure 4b refer to the deformation vibration of CH_3 and CH_2 groups. The peak at 1710 cm^{-1} is assignable to the stretching vibration of the C=O group. Compared with the peaks of kerosene (Fig. 2b) and oleic acid (Fig. 3b), the peak of synthetic collector A at 1460 cm^{-1} becomes narrower and smaller, suggesting that kerosene and oleic acid reacted with each other.

Figure 4c reveals that the adsorption peak of oil shale has shifted. For example, its deformation vibration peak has moved from 3480 cm^{-1} and 2340 cm^{-1} to 3470 cm^{-1} and 2360 cm^{-1}, respectively. It means that a weak hydrogen bond whose intensity is higher than electrostatic attraction appeared between synthetic collector A and oil shale Therefore, the

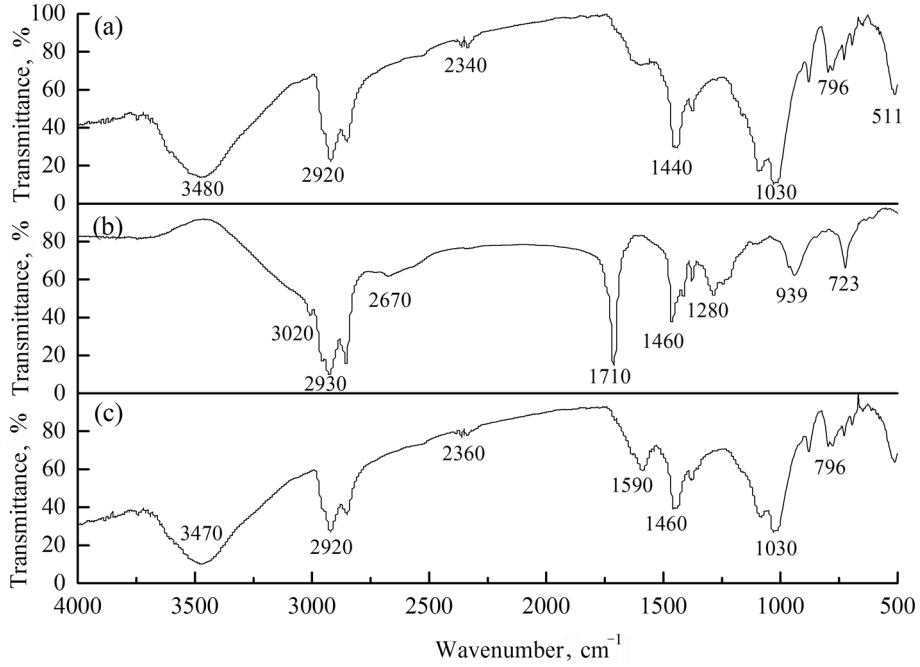

Fig. 4. FTIR spectra of (a) raw oil shale, (b) synthetic collector A, (c) oil shale infiltrated by synthetic collector A.

collecting capacity of synthetic collector A was higher even though the surface of oil shale was positively charged.

4. Conclusions

Oil shale represents the second largest solid fossil fuel deposit in the world. Due to the growing demand for alternative energy sources, improvement of oil shale quality has become a research hotspot lately. In this work, froth flotation technology was used to treat oil shale. The conclusions drawn are the following:

1. Analysis showed that treatment enhanced the utilization value of oil shale.
2. The synthetic collector exhibited the best performance when the ratio of kerosene to oleic acid was 1:1 and agitation speed 1800 rpm.
3. The flotation effect of synthetic collectors was shown to be the highest. Collector adsorption measurements indicated that with collector dosage increasing to 500 g/t, the adsorption quantity reached a relatively stable value.
4. Infrared spectroscopy measurements of raw oil shale, kerosene, oleic acid and synthetic collector A were made and the interactions between were analyzed. Synthetic collector A resulted from the reaction between kerosene and oleic acid. A weak hydrogen bond whose intensity was higher than electrostatic attraction appeared between synthetic collector and oil shale. The collecting capacity of synthetic collector A was higher than that of oil shale.

Acknowledgments

The authors acknowledge the support from the National Natural Science Foundation of China (Grant No. 51304157), the University Key Teacher by Henan Polytechnic University (Grant No. 2017XQG-12), and Henan Key Laboratory of Coal Green Conversion.

REFERENCES

1. Han, H., Zhong, N. N., Huang, C. X., Zhang, W. Pyrolysis kinetics of oil shale from northeast China: Implications from thermogravimetric and Rock-Eval experiments. *Fuel*, 2015, **159**, 776–783.
2. Jiang, H. F., Deng, S. H., Chen, J., Zhang, M. Y., Li, S., Shao, Y. F., Yang, J. Q., Li, J. F. Effect of hydrothermal pretreatment on product distribution and characteristics of oil produced by the pyrolysis of Huadian oil shale. *Energ. Convers. Manage.*, 2017, **143**, 505–512.
3. Shi, W. J., Wang, Z., Song, W. L., Li, S. G.., Li, X. Y. Pyrolysis of Huadian oil shale under catalysis of shale ash. *J. Anal. Appl. Pyrol.* 2017, **123**, 160–164.

4. Bozkurt, P. A., Tosun, O., Canel, M. The synergistic effect of co-pyrolysis of oil shale and low density polyethylene mixtures and characterization of pyrolysis liquid. *J. Energy Inst.*, 2017, **90**(3), 355–362.
5. Saif, T., Lin, Q., Bijeljic, B., Blunt, M. J. Microstructural imaging and characterization of oil shale before and after pyrolysis. *Fuel*, 2017, **197**, 562–574.
6. Miao, Z. Y., Wu, G. G., Li, P., Meng, X. L., Zheng, Z. L. Investigation into co-pyrolysis characteristics of oil shale and coal. *Int. J. Min. Sci. Technol*., 2012, **22**(2), 245–249.
7. Li, J. H., Cao, Z. B. Composition and comprehensive utilization of oil shale. *Liaoning Chem. Ind.*, 2007, **36**(6), 110–112 (in Chinese).
8. Olajossy, A. Some parameters of coal methane system that cause very slow release of methane from virgin coal beds (CBM). *Int. J. Min. Sci. Technol*., 2017, **27**(2), 321–326.
9. Gupta, N. Evaluation of graphite depressants in a poly-metallic sulfide flotation circuit. *Int. J. Min. Sci. Technol*., 2017, **27**(2), 285–292.
10. Tsai, S. C., Lumpkin, R. E. Oil shale beneficiation by froth flotation. *Fuel*, 1984, **63**(4), 435–439.
11. Altun, N. E., Hicyilmaz, C., Hwang, J. Y., Bagci, A. S. Evaluation of a Turkish low quality oil shale by flotation as a clean energy source: Material characterization and determination of flotation behavior. *Fuel Process. Technol.*, 2006, **87**(9), 783–791.
12. Altun, N. E., Hwang, J. Y., Hicyilmaz, C. Enhancement of flotation performance of oil shale cleaning by ultrasonic treatment. *Int. J. Miner. Process*., 2009, **91**(1–2), 1–13.
13. Xue, Q. H., Li, S. Y., Wang, H. Y., Zheng, D. W., Fang, C. H. Utilization of Daqing oil shale and its pyrolysis products. *Sci. Technol. Chem. Ind.*, 2009, **17**(3), 54–56 (in Chinese).
14. Hu, Y. H., Cao, X. F., Jiang, Y. R., Li, H. P., Du, P. Synthesis of N-decyl-1, 3-diaminopropanes and their structure properties for flotation of aluminosilicate minerals. *Conserv. Util. Miner. Resour.*, 2002, **22**(6), 33–37 (in Chinese).
15. Zhu, Y. M. Mineral flotation testing techniques: Measurement and application of reagents adsorption capacity on mineral surface. *Non-Ferr. Min. Metall.* 1988, **4**(2), 10–14 (in Chinese).
16. Yao, T. Y., Yao, F. Y., Li, J. S. Adsorption and adsorption enthalpy of cationic surfactant on different sand stone surfaces. *Oil Drill. Prod. Technol. 2008*, **30**(2), 82–85 (in Chinese).
17. Zang, H. C., Zang, L. X., Zhang, H., Wang, J. F., Yang, H. L., Jiang, W., Liu, D. M., Wang, F., Hu, T. Research progress on application of near-infrared spectroscopy in pharmaceuticals. *Journal of Pharmaceutical Research* 2014, **33**, 125–128.

Presented by E. Reinsalu and X. Han
Received October 1, 2017